

SEISMIC MOTION INCOHERENCY EFFECTS ON SOIL-STRUCTURE INTERACTION (SSI) AND STRUCTURE-SOIL-STRUCTURE INTERACTION (SSSI) OF NUCLEAR STRUCTURES FOR DIFFERENT SOIL SITE CONDITIONS

Dan M. Ghiocel ¹

¹ Chief of Engineering, Ghiocel Predictive Technologies, Inc., New York, USA

ABSTRACT

The paper investigates the effects of motion incoherency (3D random wave propagation) on seismic responses of nuclear structures with a focus on the seismic SSSI analysis. Basic theoretical aspects are briefly reviewed. Two NPP case studies are investigated. The incoherency effects are computed for both the single, standalone structure SSI models and the multiple structure SSSI models. The paper considers both rock and soil sites. The incoherent analyses were performed using stochastic simulation. Comparative SSI and SSSI responses include acceleration in-structure response spectra (ISRS), structural forces and moments. It is shown that the motion incoherency could amplify significantly SSSI effects for the soil sites. The seismic SSSI effects could impact significantly on the ISRS, soil pressures and bending moments in basement walls and slabs.

MODELING OF SEISMIC MOTION INCOHERENCY

The 1D seismic wave propagation assumption has been accepted in the nuclear engineering practice over the last few decades. Based on the 1D or vertically propagation assumption, the *coherent motion* at the ground surface is described by a “rigid body” motion in horizontal plane for which all the soil point motions under the foundation footprint have identical motions. In contrast to simplified representation of seismic wave field by coherent motion, the *incoherent motion* is a more accurate representation of the seismic random wave field that realistically includes the 3D seismic wave propagation aspects. Incoherent motions implicitly incorporate randomly inclined body waves and surface waves since they are developed based on real data from the dense array statistical earthquake records. Incoherent motions represent realistic 3D wave motion simulations based on the stochastic models which are developed from real record databases (Figure 1). Thus, incoherent motions include a much more realistic idealization of seismic ground motion than coherent motions. To capture this spatial variability of the ground motion, an adequate stochastic field model is required. Assuming that the spatial variation of the ground motion at different locations could be defined by a homogeneous/stationary Gaussian stochastic field, then, the spatial variability is completely defined by its coherency spectrum or coherence function.

Incoherent Free-Field Motion

The coherent free-field motion at any interaction node dof k, $U_k^{g,c}(\omega)$ is computed by:

$$U_k^{g,c}(\omega) = H_k^{g,c}(\omega)U_0^g(\omega) \quad (1)$$

where $H_k^{g,c}(\omega)$ is the (deterministic) complex coherent ground transfer function vector at interface nodes and $U_0^g(\omega)$ is the complex Fourier transform of the control motion.

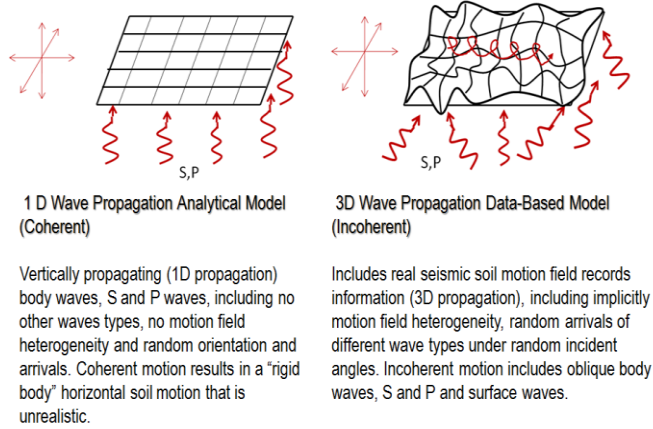


Figure 1 Coherent vs. Incoherent Soil Motion

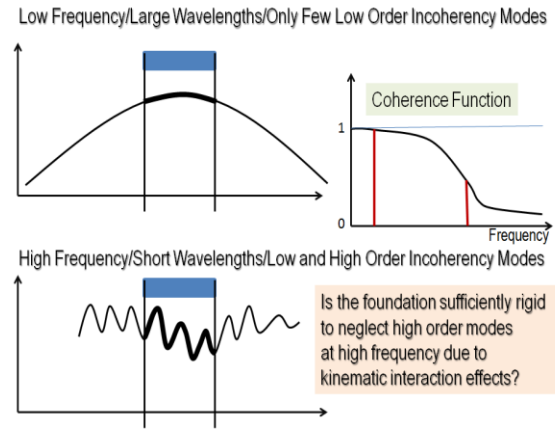


Figure 2 Low and High Frequency Soil Waves

Similarly, the incoherent free-field motion at any interaction node dof k, $U_k^{g,i}(\omega)$ is computed by:

$$U_k^{g,i}(\omega) = \tilde{H}_k^{g,i}(\omega)U_0^g(\omega) \quad (2)$$

where $\tilde{H}_k^{g,i}(\omega)$ is the (stochastic) incoherent ground transfer function vector at interaction node dofs and $U_0^g(\omega)$ is the complex Fourier transform of the control motion. The main difference between coherent and incoherent free-field transfer function vectors is that $H_k^{g,c}(\omega)$ is deterministic quantity while $\tilde{H}_k^{g,i}(\omega)$ is a stochastic quantity (the tilda represents a stochastic quantity). The $\tilde{H}_k^{g,i}(\omega)$ quantity includes deterministic effects due to the vertically propagating body waves adjusted to incorporate the stochastic motion spatial variation effects in the horizontal plane. Thus, the incoherent free-field transfer function at any interaction node can be defined by:

$$\tilde{H}_k^{g,i}(\omega) = S_k(\omega)H_k^{g,c}(\omega) \quad (3)$$

where $S_k(\omega)$ is a frequency-dependent quantity that includes the effects of the stochastic spatial variation of free-field motion at any interaction node dof k due to incoherency. In fact, in the numerical implementation based on the complex frequency approach, $S_k(\omega)$ represents the complex Fourier transform of relative spatial random variation of the motion amplitude at the interaction node dof k due to incoherency. Since these relative spatial variations are random, $S_k(\omega)$ is stochastic in nature. The stochastic $S_k(\omega)$ can be computed for each interaction node dof k using the *spectral factorization* of coherency matrix computed for all SSI interaction nodes. For any interaction node dof k, the stochastic spatial motion variability transfer function $\tilde{H}_k^{g,i}(\omega)$ in complex frequency domain is described by the product of the stochastic eigen-series expansion of the spatial incoherent field times the deterministic coherent ground motion complex transfer function:

$$\tilde{H}_k^{g,i}(\omega) = \left[\sum_{j=1}^M \Phi_{j,k}(\omega)\lambda_j(\omega)\eta_{0j}(\omega) \right] H_k^{g,c}(\omega) \quad (4)$$

where $\lambda_j(\omega)$ and $\Phi_{j,k}(\omega)$ are the j-th eigenvalue and the j-th eigenvector component at interaction node k. The factor $\eta_{0j}(\omega)$ is the random phase component associated with the j-th eigenvector that is given by $\eta_{0j}(\omega) = \exp(i\theta_j)$ in which the random phase angles are assumed to be uniformly distributed over the unit circle.

Incoherent SSI Response Calculations

For incoherent motion input, the complex Fourier SSI response at any structural dof i , $U_i^{s,i}(\omega)$, is computed similarly by the superposition of the effects produced by the application of the incoherent motion input at each interaction node dof k :

$$U_i^{s,i}(\omega) = \sum_{k=1}^N H_{i,k}^s(\omega) U_k^{g,i}(\omega) = \sum_{k=1}^N H_{i,k}^s(\omega) \left[\sum_{j=1}^M \Phi_{j,k}(\omega) \lambda_j(\omega) \eta_{0j}(\omega) \right] H_k^{g,c}(\omega) U_0^g(\omega) \quad (5)$$

Based on the approximation of the above equation, various incoherent SSI prediction approaches, from refined stochastic approaches to simple deterministic approaches, were implemented.

The number of coherency matrix eigenvectors or incoherent spatial modes depends on the eigen-series convergence. The higher the foundation flexibility is and the higher the frequency of interest is, the larger number of incoherent modes is (see Figure 2). For the “rigid” basemats, the higher-order incoherent modes are filtered out due to the kinematic SSI. However, for elastic foundations, the higher-order modes are not filtered out, and therefore, they should be included in the SSI analysis. If only a limited number of incoherent spatial modes are used, then, the incoherent SSI response could be highly inaccurate (Ghiocel, 2014). Figure 3 shows the vertical ISRS computed at the basemat of a typical NI complex using the SRSS approach (Short, Hardy, Merz and Johnson, 2007) with 20 and 40 incoherent modes, respectively. The ISRS results indicate an underestimation of the ISRS peak amplitude of up to 65% for 20 incoherent modes and up to 25% for 40 incoherent modes in comparison with the mean ISRS computed using the reference stochastic simulation approach. In vertical direction, all foundations appears to be flexible due to the reduced stiffness of their baselabs for the out-of-plane bending.

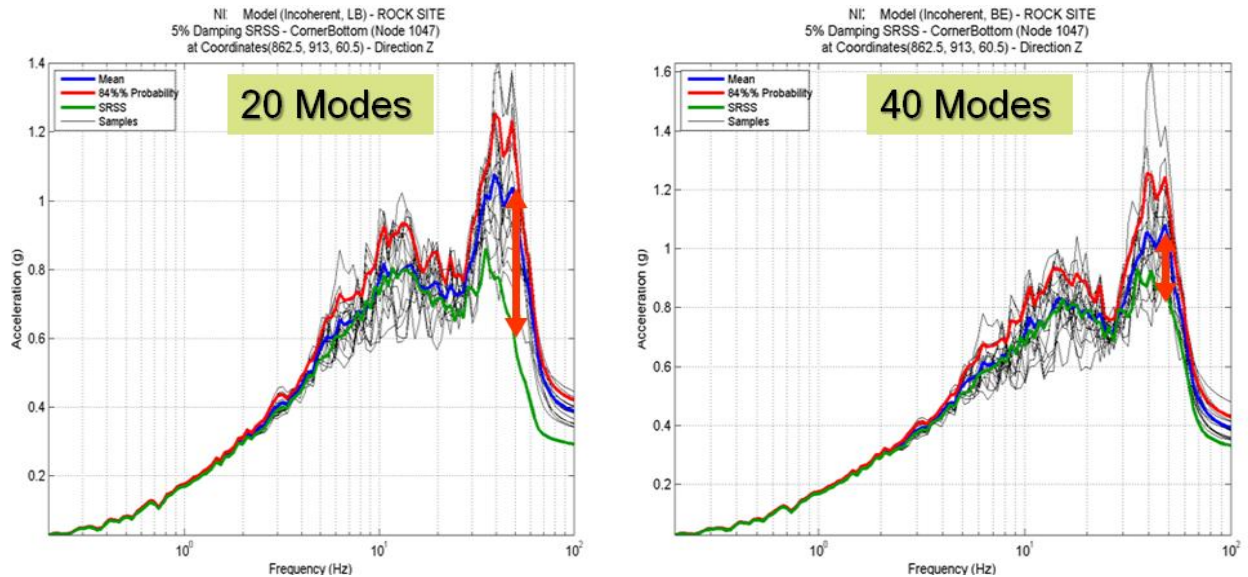


Figure 3 Effect of Number of Incoherent Modes on the ISRS Computation Using SRSS Approach

In US, EPRI investigated different incoherent SSI approaches for their application to the new nuclear power plant design within the United States (Short, Hardy, Merz and Johnson, 2007). *Stochastic approach* is based on simulating incoherent motion field random realizations. Using Stochastic Simulation (Simulation Mean in EPRI studies) algorithm, a set of incoherent motion random samples are generated at the SSI interaction nodes. For each incoherent motion sample, an incoherent SSI analysis is performed. The mean SSI response is obtained by statistical averaging of SSI response random samples. *Deterministic approaches* used were based on using simple superposition rules of random incoherent

mode effects, such as the Algebraic Sum (AS in 2007 EPRI studies) or the Square-Root of the Sum of Square (SRSS in 2007 EPRI studies), to approximate the mean incoherent SSI motion. To limit the computational efforts, SRSS is typically used with a reduced number of incoherent modes, and, therefore, applicable only to very-very stiff foundations. It should be noted that the EPRI validated incoherent SSI approaches are based on the simplification assumption that the incoherent complex motion phases are zero, or very close to zero, and therefore they are neglected. From a physical modeling point of view this not true, but, this makes the EPRI validated approaches be conservative with respect to the incoherent ISRS response computation. The zero-phase assumption produces a slightly conservative solution for simple stick SSI models as the AP1000 stick SSI model used in the 2007 EPRI validation studies (Short, Hardy, Merz and Johnson, 2007). More recent EDF studies (Zentner and Devesa, 2011) also used a deterministic SSI approach based on the zero-phase assumption that was implemented in the Code_Aster software, which is theoretically equivalent to the AS approach in the EPRI studies. However, the zero-phase assumption can provide sometimes a biased solution, especially for large-size elastic foundation models (Ghiocel, 2014). A significant practical limitation of the EPRI zero-phase approaches is that the SSI response time histories are not usable for multiple time-history analysis of the secondary systems. The cross-correlation between SSI motions at different locations are largely affected by zeroing the SSI motion phases. In the ACS SASSI code (2015), on purpose, if the complex response phase-adjustment is selected, then no acceleration or relative displacement time-history can be computed. This is to protect analyst from obtaining inaccurate results.

It should be understood that for more realistic SSI FE models with elastic basemats, rather than “rigid” basemats, the existing deterministic SSI approaches based on the zero-phase assumption, applied either at the input level for the incoherent mode combination as in AS or at the complex modal response level as in SRSS, always loose some SSI physics, and, therefore, should be always suspected for potentially producing crude results (Ghiocel, 2014). For general cases, a “theoretically exact” modeling should be based on stochastic simulation in conjunction with multiple sets of input acceleration histories and no phase adjustment. Basically, the stochastic simulation is the standard Monte Carlo simulation approach (accepted in all engineering fields) applied to quantify the motion incoherency uncertainty effects on the SSI and SSSI responses. Unfortunately, such a stochastic simulation approach with multiple input acceleration sets and without any phase adjustment, as suggested here, did not get yet sufficient exposure in the nuclear engineering community to be promoted as a “consensus” approach for performing incoherent SSI and SSSI analyses. The stochastic simulation approach applied with no phase adjustment gets rid of the artificial intrusion in the dynamic SSI physics.

In this paper we focused on a practical aspect that was apparently not sufficiently investigated so far, that addresses the effects of the motion incoherency on the seismic SSSI between neighboring nuclear structures. It should be noted that for the incoherent SSSI problems, the only reasonable approach that does not distort the SSSI coupling effects is the *stochastic simulation with no phase adjustment* that captures accurately the differential motion phasing for all foundation points.

CASE STUDIES

In this paper two incoherent SSSI analysis case studies. Both standalone SSI and SSSI FE models were considered. The two SSSI models include different NPP layouts as shown in Figures 4 and 5.

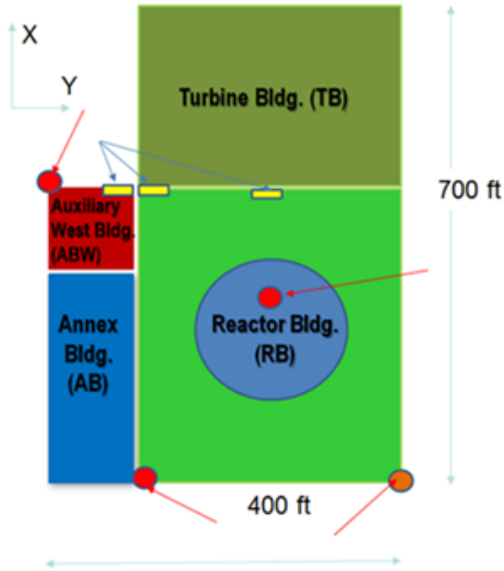


Figure 4 SSSI Model 1 of RB-TB-AB-ABW

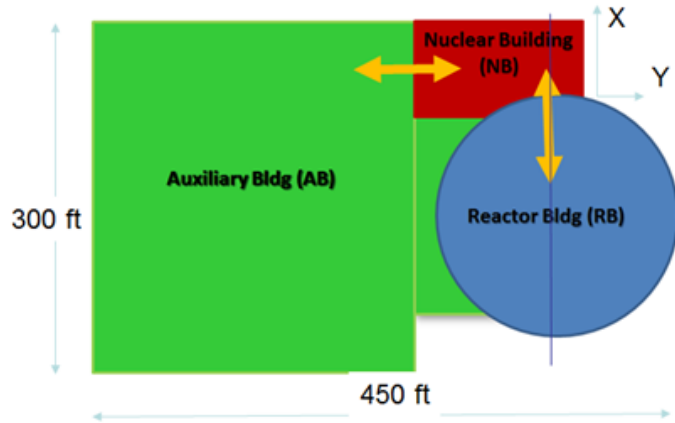


Figure 5 SSSI Model 2 of RB-AB-NB

The SSSI Model 1 includes four nuclear buildings, Reactor Building complex, Turbine Building complex and two Annex Buildings (RB, TB, AB and ABW) over a horizontal area of about 400ft x 700ft. The SSSI Model 2, includes three nuclear buildings, Reactor Building structure, Auxiliary Building and another Nuclear Building (RB, AB and NB) over a horizontal area of about 300ft x 450ft. It should be noted that in the SSSI Model 1 all buildings are surface or shallowly embedded. In contrast, in the SSSI Model 2, the RB structure is deeply embedded, while AB and NB structures are only shallowly embedded. For all coherent and incoherent SSI and SSSI analyses the ACS SASSI software (2015) was used.

SSSI Model 1 RB-TB-AB-ABW:

This SSSI model was used for two soil site conditions, named “Soil” and “Rock”, which are shown in Figures 6 and 7. The incoherent SSSI analysis used the 2007 Abrahamson generic coherency function models for soil and rock sites. The seismic input ZPGA was 0.30g for the Soil site and 0.50g for Rock site as illustrated by the spectral plots in Figure 6.

Figures 8 and 9 show the coherent and incoherent 5% damping ISRS computed at the top of the ABW structure for the standalone SSI model and the SSSI coupled model for both the Rock site (Figure 8) and Soil site (Figure 9). As expected, for the Rock site the SSSI effects are minimal, while the incoherency effects are significant. However, for the Soil site, in Y-direction, the SSSI effects show that basically the dynamic behaviour of the ABW structure is totally changed due to the adjacent RB complex. The ABW ISRS peak at 4 Hz is split in two peaks at slightly lower and higher frequencies due to the SSSI coupling with the RB complex. Also, the incoherency effects amplify the coherent SSSI ISRS peak amplitude at @ 6 Hz by about 25-30%. In the vertical Z-direction, the SSSI effects are also quite visible.

Figure 10 shows the effects of motion incoherency on the SSSI effects of the RB complex. The plots show the ISRS computed at a critical location at the top of the Internal Structure (IS). As expected, for the Rock site (upper plots) the SSSI effects are minimal, while the incoherency effects are significant. However, for the Soil site (lower plots), in the Y-direction, the SSSI effects show that basically the

dynamic behaviour of the RB complex structure is significantly changed @ 6 Hz frequency. The new ISRS peak at @ 6 Hz in Figure 10 occurs for incoherent SSSI and does not exist for coherent SSSI.

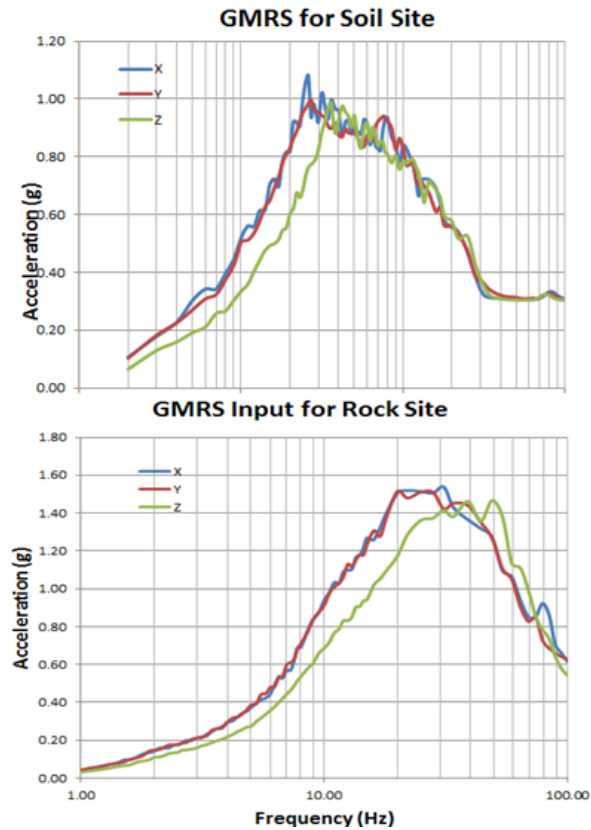


Figure 6 Site-Specific GMRS Inputs

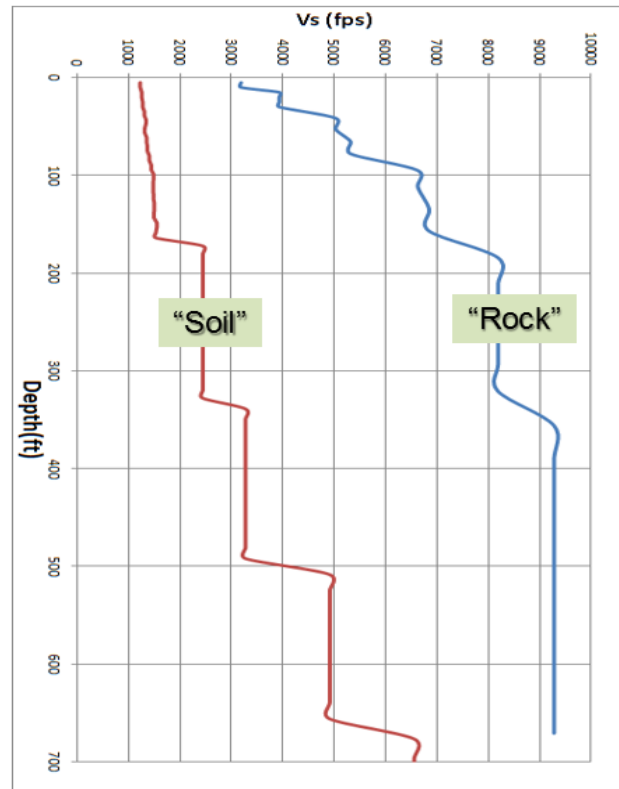


Figure 7 Vs Soil Profiles and Rock Site Conditions

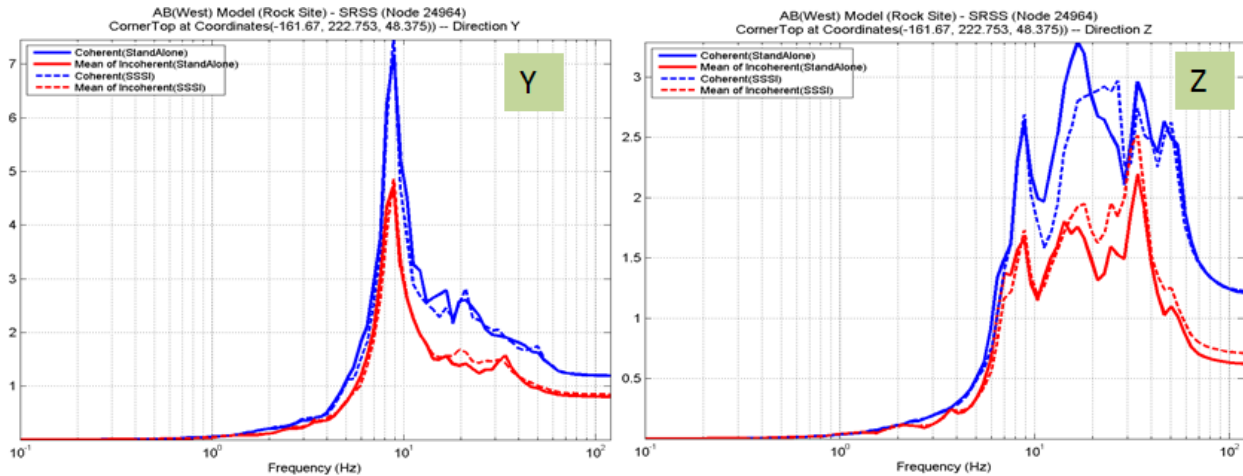


Figure 8 Coherent and (Mean) Incoherent ISRS Based on ABW SSI and SSSI Models for Rock Site

The new ISRS peak is due to the fact that the incoherent motion excites some of the RB structure local and antisymmetric vibration modes which are "dormant" under coherent SSSI. The incoherent SSSI ISRS peak amplitude at @ 6 Hz is about 100% higher than the coherent SSSI ISRS amplitude at same

frequency. This is an important practical aspect for the NPP seismic SSI analysis that is not fully recognized at this time.

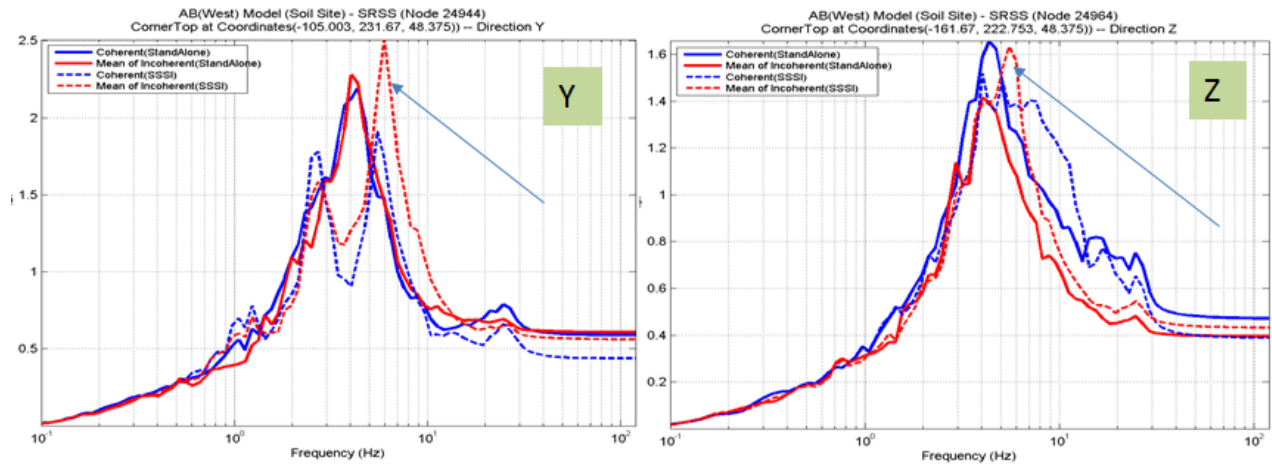


Figure 9 Coherent and (Mean) Incoherent ISRS Based on ABW SSI and SSSI Models for Soil Site

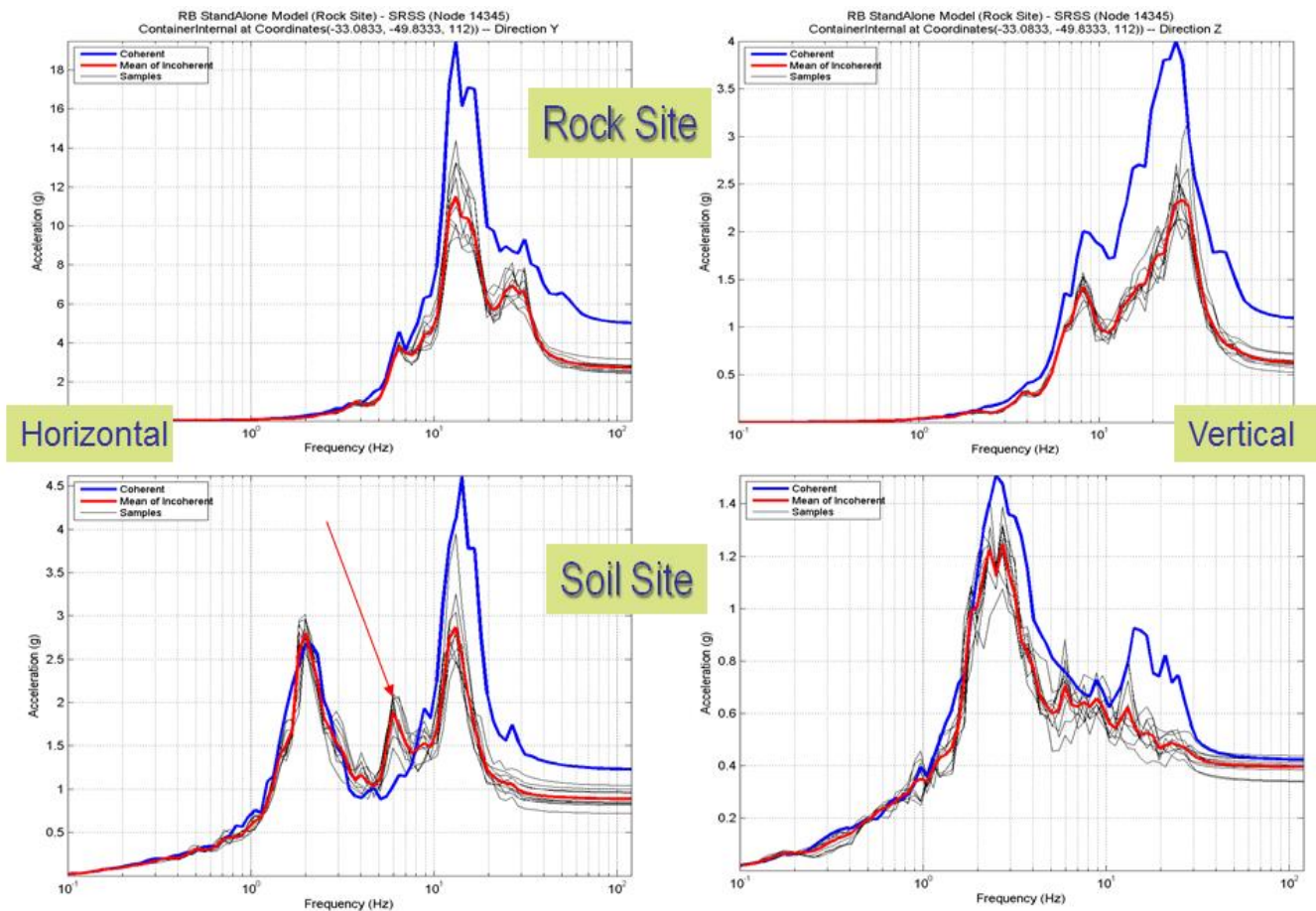


Figure 10 Coherent and (Mean) Incoherent ISRS Based on RB SSSI Models for Rock and Soil

Figures 11 and 12 show the out-of-plane (o-p) bending moments in the ABW and RB complex walls computed in the vicinity of the neighboring building based on the SSSI analyses. The coherent o-p bending moments are plotted with blue color, while the (mean) incoherent o-p bending moments are

plotted with brown color. Figure 11 shows that for the Rock site for the incoherent SSSI there is an increase of the o-p moments for the embedment part of the walls, and a reduction above ground level. However, for the Soil site, the o-p moment increases due to motion incoherency are extremely large, well above 100%.

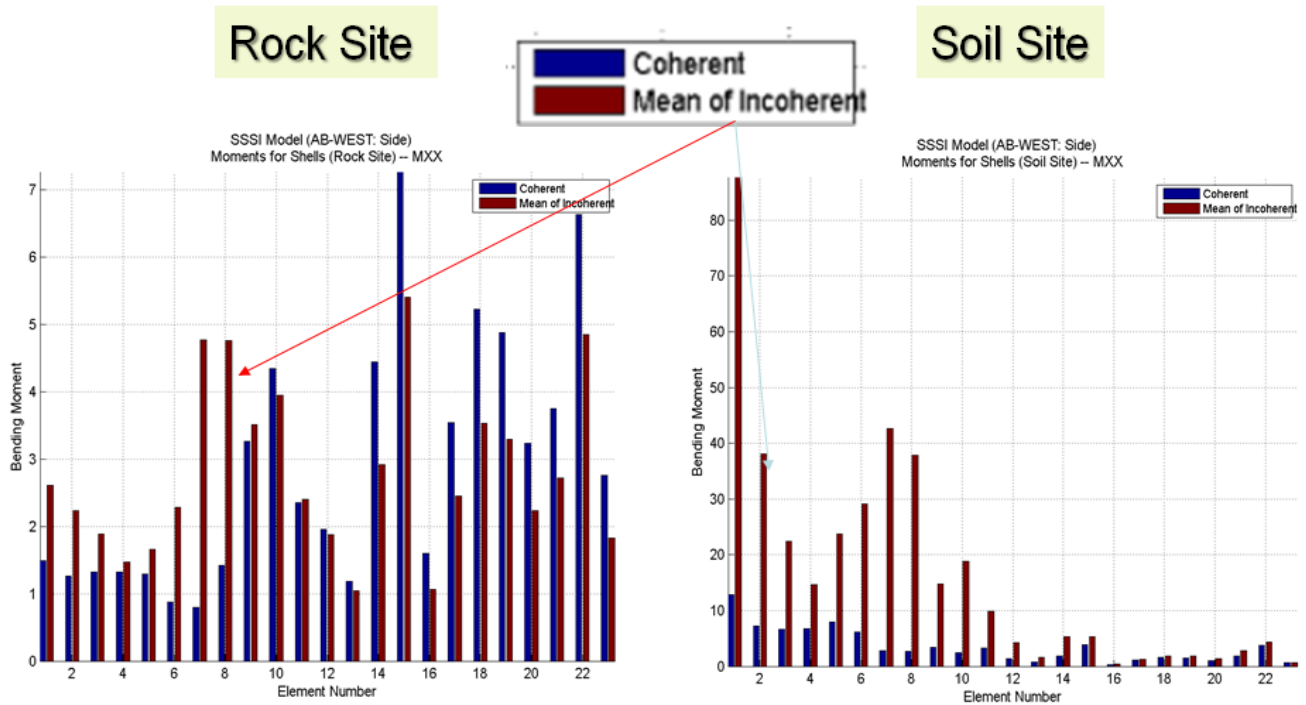


Figure 11 Out-of-Plane Moments in ABW Walls in Vicinity of RB Complex (From Foundation to Roof)

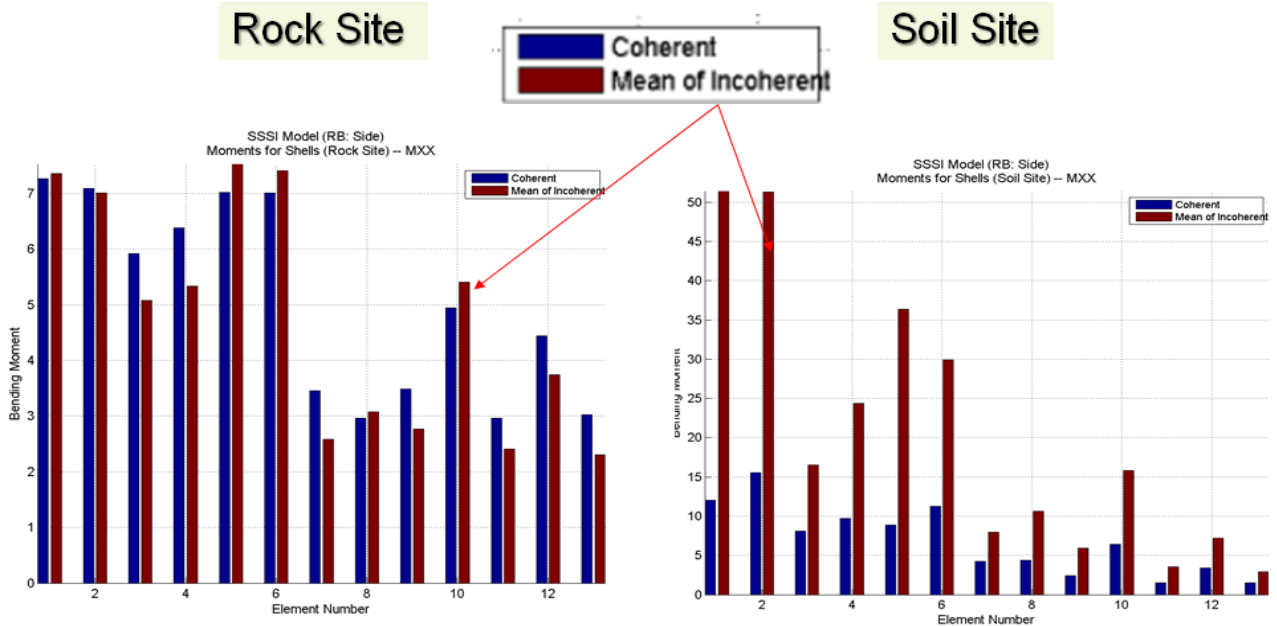


Figure 12 Out-of-Plane Moments in RB Walls in Vicinity of ABW (From Foundation to Roof)

Figure 12 indicates that for the RB walls, for the Soil site, the incoherent SSSI effects are much larger than the coherent SSSI effects. *This important aspect was often overlooked in the past due to the lack of sufficient reliable and efficient computational SSI modelling and analysis capabilities.*

SSSI Model 2 RB-AB-NB:

The investigated case study is for site with a deep soil profile having the soil Vs values varying in the 800-1500 fps range for the top 500ft depth. The seismic input motion is based on a site-specific FIRS input at the basemat of the RB structure at the depth of about 50ft. The NB and AB have shallower embedments of about 20ft depth. The site-specific in-column FIRS motions to be used for SSI and SSSI analyses were obtained based on site response analysis with the outcrop FIRS motion as input.

Figure 13 shows a comparison between the 5% damping ISRS computed at the top of the NB structure based on standalone SSI and SSSI analyses for coherent inputs. It should be noted that the SSSI NB ISRS are reduced in X-direction due to the NB base motion constraint produced by the presence of the adjacent deeply embedded RB structure, and amplified in the Y-direction due to the influence of the torsional motion of the large-size AB structure with very stiff basement that has significant mass eccentricities.

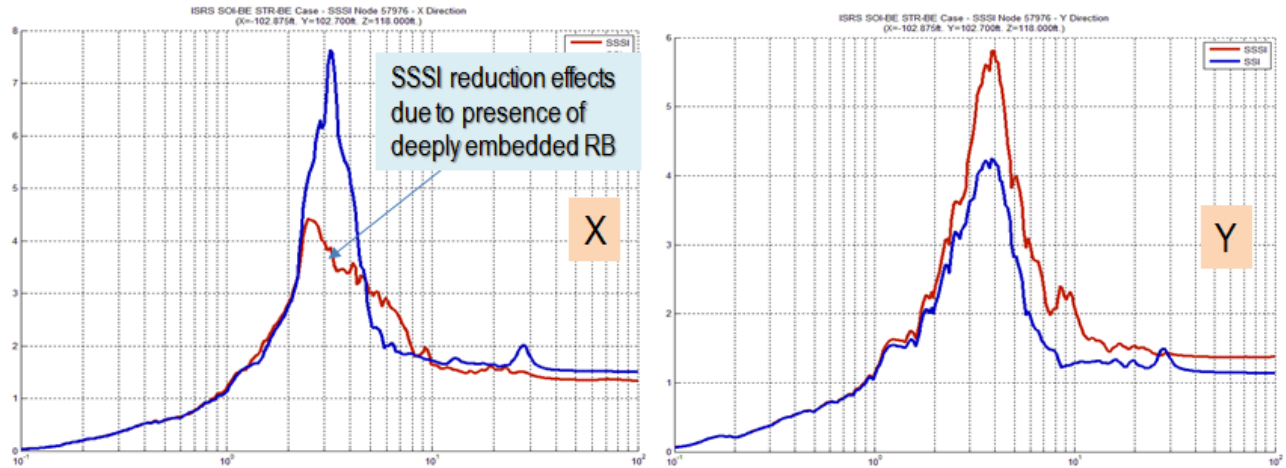


Figure 13 Horizontal ISRS for NB Standalone SSI Model (blue line) and SSSI Model (red line)

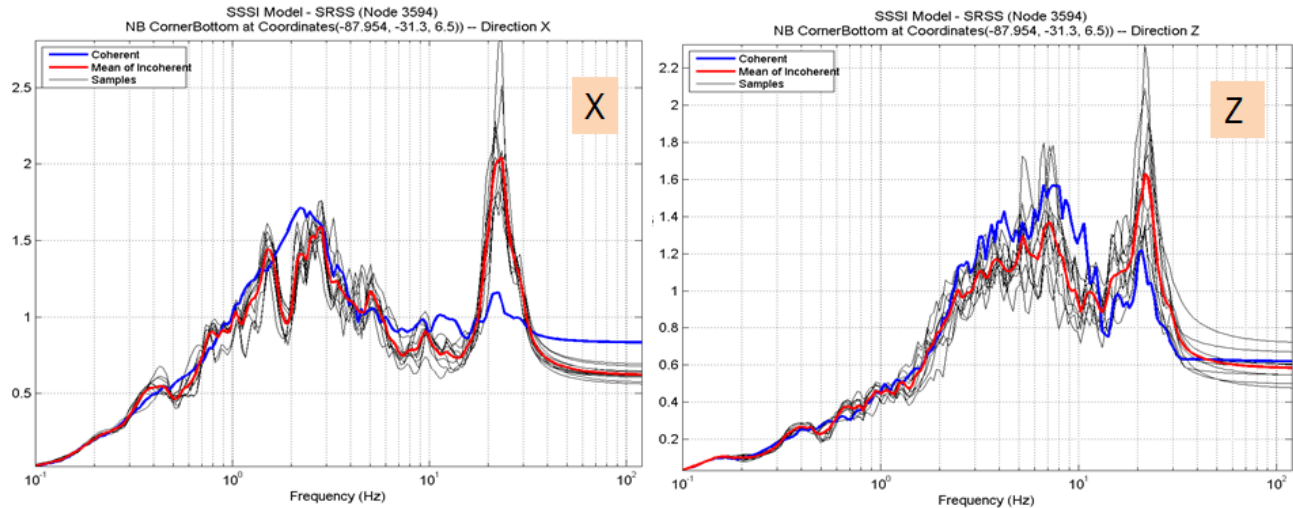


Figure 14 Horizontal and Vertical Coherent ISRS (blue) and (Mean) Incoherent ISRS (red) for NB SSSI Model at Basemat Corner near RB Foundation

Figure 14 shows a comparison of the coherent ISRS and incoherent ISRS computed from the SSSI analysis at the NB basemat corner near the RB foundation. The incoherent SSSI effects were the largest for this ISRS location. The high-frequency SSSI mode at @ 20.0 Hz that was “dormant” for the coherent

SSSI analysis is largely amplified, about 100%, for the incoherent SSSI analysis. The dynamic coupling between the NB structure and RB structure is significantly excited by the incoherent motion.

The seismic soil pressures on the NB baseslab computed based the standalone SSI and SSSI analysis are shown in Figure 15. The seismic pressure contour plots show large soil pressure amplifications at the edge of the NB baseslab close to the RB foundation. The RB foundation restricts the motion of the NB foundation. For such situation, it is possible that the surrounding soil nonlinear local behavior might play a significant role on SSSI effects, especially for incoherent motions that could produce larger amplification of scattered waves. Additional ACS SASSI nonlinear analyses are underway.

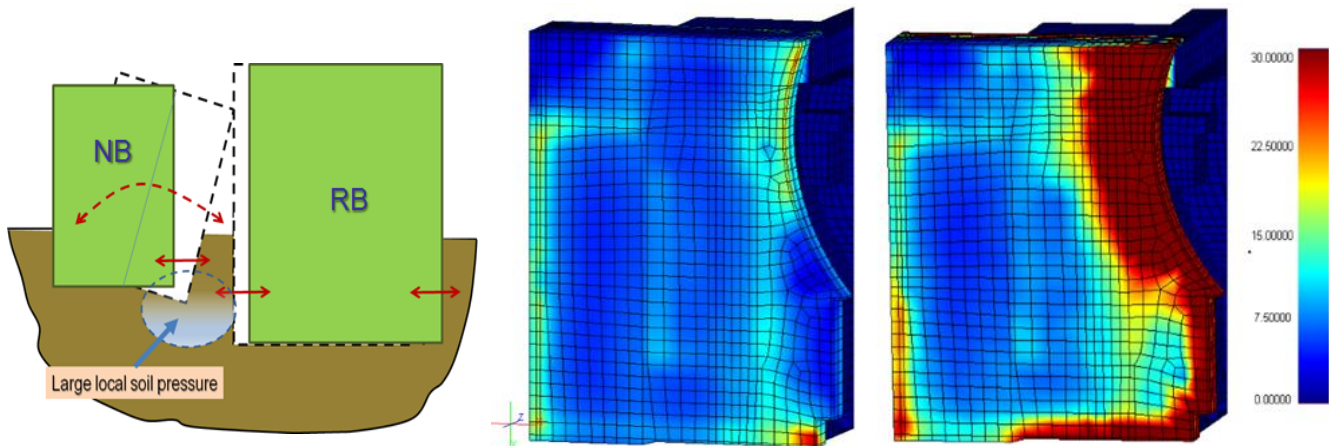


Figure 15 Seismic Soil Pressures on NB Baseslab for Standalone SSI Model (left) and SSSI (right)

CONCLUSIONS

The paper investigates the seismic motion incoherency effects on the SSI and SSSI responses using a state-of-the-art stochastic FEA modeling via stochastic simulation. It is shown the motion incoherency could play a significant role for SSSI effects, especially for soft soil sites by largely amplifying the ISRS and the basement soil pressures (and bending moments).

REFERENCES

Ghiocel D, M. (2014). "Effects of Seismic Motion Incoherency on SSI and SSSI Responses of Nuclear Structures for Different Soil Site Conditions", U.S. Department of Energy, DOE Natural Phenomena Hazards Meeting, Session on "Soil-Structure Interaction", Germantown, MD, USA, October 21-22
<http://www.energy.gov/sites/prod/files/2015/05/f22/DOE-NH-Motion-Incoherency-SSI-SSSI-Oct-21-2014.pdf>

Ghiocel Predictive Technologies, Inc. (2015). "ACS SASSI - An Advanced Computational Software for 3D Dynamic Analyses Including SSI Effects", ACS SASSI Version 3.0 Manuals, March 31,
http://www.ghiocel-tech.com/enggTools/ACS%20SASSI_V300_Brief_Description_Dec_31_2014.pdf

Short, S.A., G.S. Hardy, K.L. Merz, and J.J. Johnson (2007). "Validation of CLASSI and SASSI to Treat Seismic Wave Incoherence in SSI Analysis of Nuclear Power Plant Structures", Electric Power Research Institute, Palo Alto, CA and US Department of Energy, Germantown, MD, Report No. TR-1015111, November